

CLEAN UP OF MALACHITE GREEN DYE IN AQUEOUS SOLUTION USING ZnO NANOPOWDER

H. IDRIS^{a,b,*}, A. ALAKHRAS^a

^a*Deanship of Scientific research, Imam Mohammad Ibn Saud Islamic University (IMSIU), KSA*

^b*Sudan Atomic Energy Commission*

Malachite green dye has been known to have toxic carcinogenic characteristics and potential health risks for humans even at low concentrations. Hence, it is very vital to remediate the dye before discharge into water bodies or water treatment systems. Thus, this article demonstrated the removal of cleanup of malachite green (MG) dye from the aquatic phase using ZnO nanopowder. In this work batch adsorption experiments were accomplished as a function of contact time, pH, and initial dye concentration to study the efficiency of ZnO nanopowder on dye removal (MG). The obtained nanopowder was characterized using various techniques XRD, FTIR, SEM and EDX. The results shown that the maximum absorbed value was 233.16 mg / g. The findings show that ZnO nanopowder have fast contact time and initial concentration absorbing characteristics in dye removal. The maximum capacity of sorbent was found to be 246.36 mg. Furthermore, the study revealed that ZnO nanopowder is an effective sorbent for cleanup of malachite green dye in aqueous solution when comparing with other adsorbent materials. The Adsorption and kinetics parameters of the maximum capacity of sorbent and correlation coefficient showed that the data were well fitted the to the Langmuir isotherm R² of 0.923 models and pseudo-second-order kinetic model with R² of 0.994 respectively.

(Received August 18, 2020; Accepted November 6, 2020)

Keywords: Adsorption, Characterizations, Isotherm, Kinetics, ZnO nanopowder

1. Introduction

Water pollution has become an important issue that worries societies as a result of population growth, industrial revolution, and water demand [12]. Dyes are a type of pollutant that can appear in wastewater due to the activities of industries including stones, pigment, variegated, cosmetics and textiles [7]. It is well documented that in the literature malachite green (MG) dye poisonousness and have carcinogenic properties and possible health risk for humans even at low concentration 1 mg / l. [3]. Dyes can decrease light diffusion into the aquatic ecosystems; so it has an adverse impact on vegetation and biota. Furthermore, eliminating these sorts of stains and compounds is essential due to their toxicity and health risk. Therefore, the remediation of dyes from wastewater and sewerage is necessary and unavoidable [6,37]. Although, scientists have examined various approaches, such as ozonization, reverse osmosis, oxidation, coagulation and sedimentation for eliminating the dye in agnatic system [29,5,30] However, these traditional methods are not sufficiently adequate to remediate the dye because of many factors, which include cost and efficiency. Recently, efforts have been performed to utilize nanoparticles, particularly metal oxide nanoparticles, for the wastewater remediation [13]. These metal oxides hold novel characteristics like wide surface area, huge adequacy, and highly chemical stabile [32]. Hence, these metal oxides nanoparticle might be the appropriate and effective adsorbents for dye treatment. Among those nanoparticle, ZnO is common broadly used because of its chemical stability, environmentally safe, cost-effective, and its ability to provide a massive number of reactive radicals [14,17,1]. The current work intended to study removal efficiency of malachite green by ZnO nanopowder in aqueous solution.

* Corresponding author: hjoidriss@gmail.com

2. Materials and methods

2.1. Production of ZnO nanopowder

For ZnO nanopowder (ZnO – NP) production, 100 mL of zinc nitrate dehydrate (of 0.3 M) solution was agitated for 30 min. (100 mL) pectinose (33.3 mmol) was added drop by drop to the solution of zinc nitrate under strong stirring for 6 h at 90 °C. Afterward, the received white powder was cooled at ambient condition and then milled and annealed at 400 °C for 3 h to achieve ZnO nanopowder as synthesis by [12]. The obtained nanopowder was studied using various techniques.

2.3. Adsorption equilibrium

Stock solution of MG dye (500 ppm) was prepared using distilled water and stored in dark at room temperature. then, 10 ml of MG with concentrations 50, 100, 200, 300, 400 and 500 ppm were added to 0.03 g of ZnO – NP at room temperature and agitated by shaker (250 rpm) for 6 hours and pH 3 kept constant. After the experiment ended, the solution was removed from the adsorbent using filter paper and analyzed by the UV - Vis spectrophotometer (620 nm λ max). The quantity of MG adsorbed by (ZnO – NP) at time) qt) was calculated by the formula (1). After the test ended, the solution was removed from the adsorbent using filter paper and analyzed using UV- Vis spectrophotometer (620 nm). The quantity of MG adsorbed by (ZnO – NP) at time) qt) was calculated by the formula (1).

$$q_t = \frac{V(C_0 - C_t)}{m} \quad (1)$$

where, q_t (mg g^{-1}) is mass of dye adsorbed by a unit mass of nanopowder m (g) at time t (min), V is the solution volume (L), C_0 concentration of the metal ion initially preset and C_t is that at time in (mg L^{-1}). Furthermore, the removal percentage (%) of the MG by adsorption at time(t) can be determined by equation (2).

$$\text{removal}(\%) = \frac{(C_0 - C_t)}{C_0} \times 100 \quad (2)$$

2.2. Adsorption kinetic

The adsorption kinetic was achieved using (ZnO – NP) (0.05g) and 200 ppm MG concentration mixed together in 50ml Erlenmeyer Flask and agitated by shaker (250 rpm).The solution was extracted from the adsorbent using filter paper at a different times 20,40,60,80,100 and 120 min and measured using the UV - Vis spectrophotometer at 620 nm. The quantity of MG adsorbed via adsorbent at equilibrium (q_e) was computed by formula (3).

$$q_e = \frac{V(C_0 - C_e)}{m} \quad (3)$$

3. Result and discussion

3.1. XRD analysis of ZnO nanopowder

The characterization of ZnO nanopowder was carry out using X-ray Diffractometer. The XRD structure of ZnO nanopowder which is fabricated at 700 °C for 3 h is displayed in Fig. 1. From the figure it can be seen that the broad peaks at position (31.79, 34.22, 36.13, 47.43, 56.52, 62.74 ,66.44, and 67.94 deg. as 2 theta) was recorded. Obviously, these measurable peaks are determined as (100), (002), (101), (102), (110), (103), (200), (112), (201), (004) and (202) plans of which can be classified to ZnO wurtzite structure (Kołodziejczak-Radzimska and Jesionowski 2014).

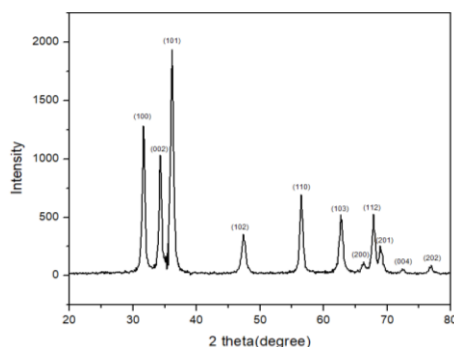


Fig. 1. XRD pattern of ZnO nanopowder fabricated at 400 °C for 3 h.

The Lattice Geometry equation was used to calculate the d-spacing, lattice parameters (a,c, c/a) and unit cell (v) of ZnO nanopowder. It was found that the value of d-spacing is (2.484), lattice parameters a (3.257), c (5.222) and c/a (1.6033) as well as the value of unit cell is (47.972). the crystallite size was computed using Scherer equation (10) [11] .

$$D = \frac{0.9\lambda}{\beta \cos \theta} \quad (10)$$

(where: D, λ , β and Θ are the crystallite size, wavelength of the X-ray source (Cu K_{α}), full width at half maximum (FWHM) and Bragg's diffraction angle respectively). The average crystallite size of the synthetic MgO nanopowder was to be 18.23.

3.2. Textural and elemental characterization

The surface morphological and elemental contains were investigated by a scanning electron microscope (Phenom XL, Netherland) at different magnifications (5 μ m, 8 μ m and 10 μ m) as shown in Fig. 2. The nanopowder are largely agglomerated and non-uniform as well as approximately similar to tree leaves as can be seen in Fig. (2a and 2c). however, the shape that was observed in fig(2b) have some porous accompanied by some babbles distributed on the surface of the nanopowder. The EDX analysis of the nanopowder is revealed that no of impurities was identified in the MgO nanopowder sample as shown in Fig. (2d).

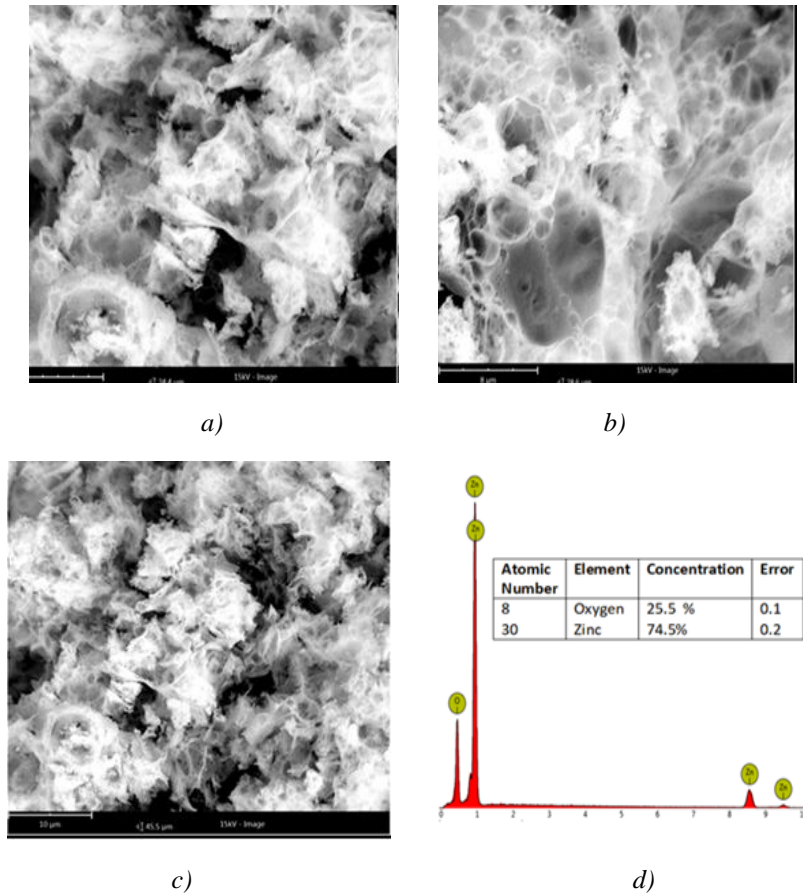


Fig. 2. SEM images of ZnO nanopowder at different magnification

(a) 5 μm , (b) 8.5 μm , 10.5 μm and EDX spectrum.

3.3. FTIR characterization

The formulation and pureness of ZnO nanopowder have been examined utilizing FTIR spectrometry in the range of (250-4000 cm^{-1}) as can be shown in Fig. 3. From the figure, it can report that the absorption was registered at peaks 451, 1625, 2346 and 3448 cm^{-1} . The dominant peak at 451 cm^{-1} refers to the expansion caused by the vibration of Zn-O mode, which approving the formation of ZnO nanopowder (Umar et al., 2015). Moreover, the peak that was recorded at 3463 cm^{-1} is due to vibration of water molecules on the ZnO nanopowder surface as well as the peak at 2346 is due to CO_2 found in the air [2].

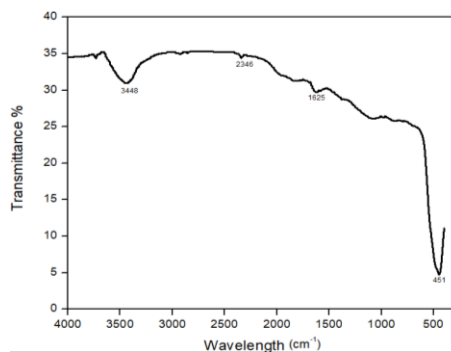


Fig. 3. FTIR spectra of synthesized ZnO nanopowder.

3.4. Effect of initial dye concentration

The investigation of the impact of initial dye concentration on the removal of MG dye by ZnO – NP was carried out in dye concentration of was studied in the dye concentration range from 50 - 500 mg/l as shown in Fig. 4. It can be noticed that from the rate of removal percentage is very high in all concentrations that were studied, and the difference in the removal percentage is almost neglected. the as the highest removal rate was 99.67 % at concentration of (200 ppm) and the lowest removal rate was 98.02 at concentration (400 ppm). This model of dye removal could be due to the existence of a large number of active sites on the surface of ZnO – NP to absorb MG dye [13].

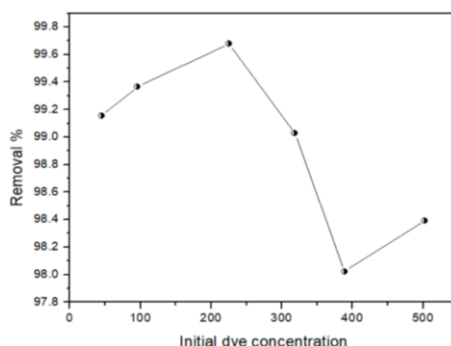


Fig. 4. Initial dye concentration as function of removal percentage %.

3.5. Effect of contact time

The influence of contact time on dye elimination via was tested to find out the equilibrium time for dye removal. Adsorption efficiency experiments were carried out with different contact times ranging from 20 - 120 min as can be seen in Fig. 5. From the figure the dye removal increased from 55.05 to 78.6 % with increase in contact time from 20 to 80 min. A rapid increase in the absorption of pigments might be owing to the accessibility of a huge amount of active sites on ZnO – NP surface for MG absorption [22,24]. After a period of time, the adsorption of dyes was slow and finally attained equilibrium. This can be attributed to the saturation on the surface of ZnO – NP surface and repulsion force construct among the MG dye molecules on ZnO – NP surface [33]. The maximum removal percentage was found to be 87.44 % at time 100 min.

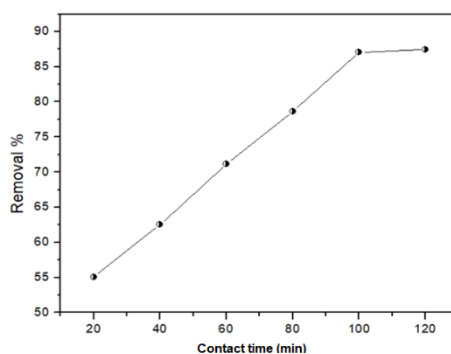


Fig. 5. Contact time as function of removal percentage %.

3.6. Effect of pH

The influence of PH on the removal of MG dye by ZnO – NP was analyzed in the PH (4, 7, 9, 10 and 11). the experimental conditions were kept constant which include (adsorbent dose 0.03 g, MG concentration 200 mg/L, temperature and contact time). Fig. 6 presents the removal percentage of MG dye by ZnO – NP. It can be seen that there is no significant variation in the removal behaviors at pH 4, 7 and 9. Another researcher has noted comparable behavior of dye

removal [13]. It is well documented in the literature at lower PH the adsorbent undergo to decomposition as well as at low pH, the electrostatic repulsion between MG dye molecules and the positively charge surface of the ZnO nanoparticles is higher that is resulting in less MG dye removal [8,38]. On the other hand, at pH 10 and 11 the removal personage is very high 95 % at pH 10 and 100 % at pH 11.

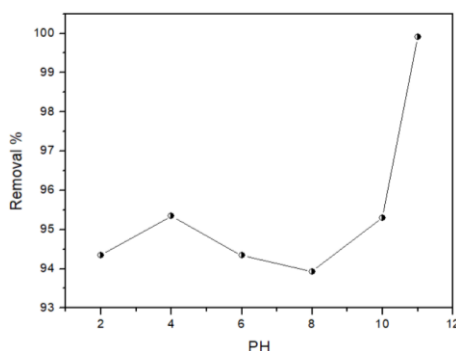


Fig. 6. pH as function of removal percentage %.

3.7. Adsorption isotherm study

The adsorption equilibrium of MG dye removal by ZnO – NP was analyzed using Langmuir and Freundlich adsorption models.

3.7.1. The Langmuir isotherm

The model is essentially implemented to explain the monolayer adsorption that occurred on the homogeneous surface of adsorbent [15].

$$\frac{C_e}{q_e} = \frac{1}{q_m} C_e + \frac{1}{q_m \cdot K_L} \quad \text{Langmuir (linear equation)} \quad (4)$$

where: C_e = the equilibrium concentration of adsorbate (mg/l-1) q_e = the amount of dye adsorbed per gram of the adsorbent at equilibrium (mg/g), q_m = maximum monolayer coverage capacity (mg/g) K_L = Langmuir isotherm constant (L/mg). q_m and K_L represent the slope and intercept of C_e/q_e versus C_e plotting.

3.7.2. Freundlich isotherm model

This model is used to describe adsorption on both homogeneous and heterogeneous surfaces [4].

$$\ln q_e = \frac{1}{n} \ln C_e + \ln K_F \quad \text{Freundlich (linear equation)} \quad (5)$$

In Freundlich equation k and n are obtained from the $\ln q_e$ against $\ln C_e$ diagram. K_F and n of the Freundlich model are associated with the adsorptive bond strength and distribution, respectively. Freundlich isotherm constant (n) is the indication of the adsorption intensity and the magnitude of n was between 1 and 10 this confirm the favorable condition for the adsorption. Langmuir isotherm constant can be explained by the equilibrium parameter (separation factor R_L), which is a constant without dimensions as described in formula 6. The value of R_L lie between 0 and 1 this indicates that the adsorption is favorable for all the initial dye concentration. The two models describe the correlation coefficient (R^2).

$$R_L = \frac{1}{1 + K_L \cdot C_0} \quad (6)$$

Fig. 7a presents the Langmuir adsorption isotherm of MG dye removal by ZnO – NP. From the obtained figure the correlation coefficient R^2 was 0.9289, while the correlation coefficient of the Freundlich isotherm was 0.879 as shown in Fig. 7b. The correlation coefficient (R^2) was used to assess the suitability of the isotherm model; the high value of (R^2) being the most appropriate. A comparison of the data of the Langmuir and Freundlich adsorption models shows that the Langmuir model is in excellent agreement with adsorption experiments data for MG dye. Table 1 shows the parameters data of isotherms models of MG dye removal by ZnO – NP. The maximum adsorption capacity (q_m) of MG dye and by ZnO – NP nanoparticles was found to be 246.36 $\text{mg}\cdot\text{g}^{-1}$. The obtained value for q_m was compared with other investigated adsorbents materials, as depicted in a Table 2. The value R_L was 0.0078 lie between 0 and 1 this means that the adsorption is favorable for all the initial dye concentration. Furthermore, the value of the Freundlich isotherm constant (n) is the indication of the adsorption intensity and the value was (1.475), the value between 1 and 10 this confirm the favorable condition for the adsorption.

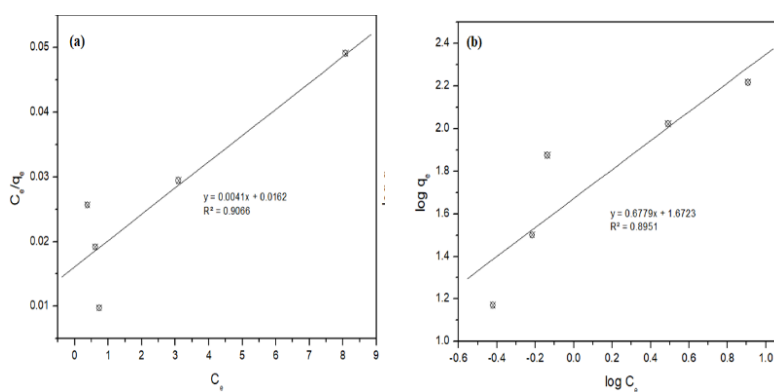


Fig. 7. (a) Plot of linearized Langmuir adsorption isotherm of MG dye by ZnO – NP:(b) Plot of linearized Freundlich adsorption isotherm of MG dye by ZnO – NP.

Table 1. Adsorption equilibrium constants for the dye removal by ZnO nanopowder.

Langmuir constants				Freundlich constants		
$q_m(\text{mg}\cdot\text{g}^{-1})$	$K_L(\text{l}\cdot\text{mg}^{-1})$	R_L	r^2	n	k_f	r^2
246.63	0.251	0.0078	0.9066	1.475	47.026	0.8951

Table 2. A summary of the comparison between the values of the adsorption capacity of ZnO nanopowder with other reported adsorbents.

adsorbent	Adsorption capacity (mg/g)	Reference
ZnO nanopowder	246.63	Current study
Metal–Organic Frame workMIL-53(Al)	164.9	[20]
Multi-walled carbon nanotube	80.64	[9]
Halloysite nanotubes	99.6	[16]
Activated carbon	27.78	[27]
Oil palm trunk fibre	149.35	[10]
Rubber wood	36.46	[19]
Jute fiber carbon	136.58	[25]
Bagasse fly ash	170.33	[21]
Ultrathin NiO nanoflakes	142.08	[34]

3.8. Kinetic study

The MG dye removal mechanism rate was evaluated applying pseudo-first- order [23], pseudo-second order [28], intraparticle diffusion [36] and Elovich model kinetic models [26]. The models are displayed in the linear formula as follows.

3.8.1. First- order

This model supposes that the adsorption rate is proportionate to the variation between q_e and q_t [40].

$$\ln(q_e - q_t) = \ln(q_e) - k_1 \cdot t \quad \text{pseudo-first- order model} \quad (7)$$

where: k_1 = rate constant (min^{-1}). From the slope and intercept of $\ln(q_e - q_t)$ against t plot, k_1 and q_e can be determined respectively. The fitting plots of pseudo-first- order kinetic models are shown in Fig. 8a. From the figure obtained the correlation coefficient R^2 was 0.957, the other kinetic parameters for the adsorption of MG onto ZnO – NP are summarized in Table 3.

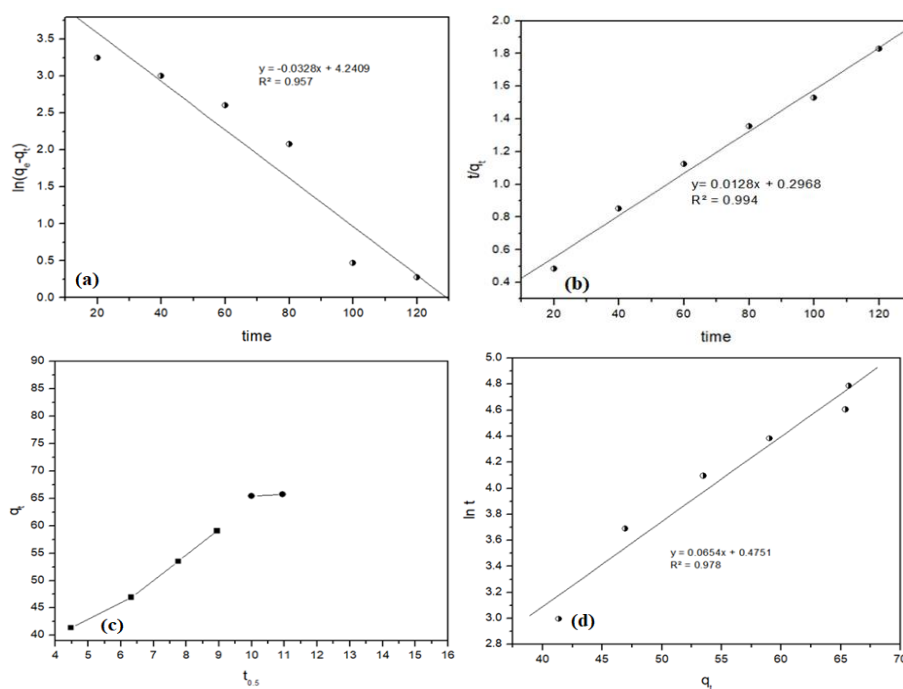


Fig. 8. (a) pseudo-first-order kinetic model for MG dye removal by ZnO – NP:(b) pseudo-second -order kinetic model for MG dye removal by ZnO – NP:(c) Intraparticle diffusion kinetic model for MG dye removal by ZnO – NP:(d) Elovich kinetic model for MG dye removal by ZnO – NP.

Table 3. Pseudo-first-order, Pseudo-Second order, Intraparticle diffusion and Elovich model. kinetic parameters for the dye adsorption by ZnO nanopowder.

Kinetic model	parameters	Value
Pseudo-first-order	q_m (experimental) ^a	67
	k_1 (g/mg min)	0.033
	q_m (calculated) ^b	69.49
	r^2	0.957
Pseudo-Second order	K_2 (g/mg min)	0.0025
	q_m (cal) ^b	77.95
	r^2	0.994
Intraparticle diffusion	K_{dif1} (mg/g min ^{0.5})	3.978
	C (mg/g)	22.87
	r^2	0.988
	K_{dif2} (mg/g min ^{0.5})	0.305
	C (mg/g)	62.43
	r^2	1.00
Elovich model	α (mg g ⁻¹ min ⁻¹)	0.609
	B (gmg ⁻¹)	0.068
	r^2	0.978

3.8.2. Pseudo-second order

In this model, the absorption operation is a chemical process that includes electron participating or electronic moving between adsorbent and adsorbate [40].

$$\frac{t}{q_t} = \frac{1}{k_2 \times q_e^2} + \frac{t}{q_e} \quad \text{pseudo-second order model} \quad (8)$$

where: k_2 denotes the rate constant (g (mg.min⁻¹)). Applying of t/q_t against t graph, q_e and k_2 are obtained from the slope and intercept. The pseudo- second- order kinetic models fitting plots was presented Fig. (8b). From the figure obtained the correlation coefficient R^2 was 0.994 , the other kinetic parameters for the adsorption of MG onto ZnO – NP listed in Table 3.

3.8.3. Intraparticle diffusion model

The model is applied to determine the potentiality of intra-particle diffusion resistance influencing adsorption [40].

$$q_t = k_{dif} \cdot t^{1/2} + C \quad \text{Intraparticle diffusion model} \quad (9)$$

At this point, k_{dif} is the intra-particle diffusion rate constant and C is constant. k_{dif} and C can be calculated from the slope and intercept by plotting the q_t against $t_{0.5}$ respectively. The fitting plots of intraparticle diffusion kinetic models was shown in figure (8c). The figure exhibited two kinds of linearity showing two diffusion steps of MG dye adsorption onto ZnO – NP. The first stage plot passed near the origin with $k_{dif1} = 3.978 \mu\text{g/g/min}^{0.5}$ while the second one did not with $k_{dif2} = 0.305 \mu\text{g/g/min}^{0.5}$. It was concluded that the second stage was controlled by both film and intraparticle diffusions. The $k_{dif1} \geq k_{dif2}$ was associated with a faster rate of film diffusion than intraparticle diffusion. It was concluded that the adsorption kinetics might be regulated by intraparticle diffusion [40].

3.8.4. Elovich model

The model is applied in adsorption kinetics to explains the chemical reaction process in nature[35].

$$q_t = \frac{1}{\beta} \ln[\alpha\beta] + \frac{1}{\beta} \ln t \quad \text{Elovich model} \quad (10)$$

Here, α = the initial adsorption rate ($\text{mg g}^{-1}\text{min}^{-1}$), β = the desorption constant (gmg^{-1}) during any one experiments. A plot of q_t against $\ln t$ will give a slope of $[1/\beta]$ and an intercept give $1/\beta \ln[\alpha\beta]$.

Fig. 8a presents the Elovich model kinetic model of MG dye removal by ZnO – NP. From the obtained figure the correlation coefficient R^2 was 0.978. The correlation coefficient (R^2) was used to evaluate between the experimental and theoretical (kinetic models) results. From the kinetic data information, the (q_e) value computed from the pseudo-first-order was 69.46 which is slightly higher than practical value 67. Nevertheless, the calculated (q_e) value from the pseudo-second-order was 77.95. From the obtained result the adsorption of MG dye via ZnO – NP is follow the pseudo-second-order kinetic model.

4. Conclusion

To sum up, eco-friendly nanoscale zinc oxide has been produced through a simple and inexpensive method. Batch adsorption experiments were accomplished as a function of contact time, PH, and initial dye concentration to study the efficiency of ZnO nanopowder on dye removal (MG). The findings show that ZnO nanopowder have fast contact time and initial concentration absorbing characteristics in dye removal. The maximum capacity of sorbent was found to be 233.16 mg. furthermore, the study revealed that ZnO nanopowder is an effective sorbent for cleanup of malachite green dye in aqueous solution when comparing with other adsorbent materials. The kinetics parameters of the maximum capacity of sorbent and correlation coefficient showed that the data were well fitted to the pseudo-second-order kinetic model with R^2 of 0.994. Therefore, it can be said that the absorption operation is a chemical process that includes electron participating or electronic moving between adsorbent and adsorbate.

Acknowledgements

The author is grateful to Dr. Abueliz Modwi for his assistance in preparing the samples

References

- [1] Rafai Abdel-Aziz, M. A. Ahmed, M. F. Abdel-Messih, *Journal of Photochemistry and Photobiology A: Chemistry* **389**, 112245 (2020).
- [2] Babiker Y. Abdulkhair et al., *Zeitschrift für Naturforschung A* **74**(10), 937 (2019).
- [3] T. K. Arumugam et al., *International journal of biological macromolecules* **128**, 655 (2019).
- [4] H. Bekhti et al., *Microporous and Mesoporous Materials* **294**, 109866 (2020).
- [5] H. Bekhti et al., *Microporous and Mesoporous Materials* **294**, 109866 (2020).
- [6] Nezamaddin Daneshvar et al., *Journal of Electroanalytical Chemistry* **615**(2), 165 (2008).
- [7] Zeinab Hosseini Dastgerdi et al., *Journal of Environmental Chemical Engineering* **7**(3), 103109 (2019).
- [8] V. K. Garg, Rakesh Kumar, Renuka Gupta, *Dyes and Pigments* **62**(1), 1 (2004).
- [9] Mehroang Ghaedi et al., *Physical Chemistry Chemical Physics* **18**(19), 13310 (2016).
- [10] B. H. Hameed, M. I. El-Khaiary, *Journal of hazardous materials* **154**(1-3), 237 (2008).
- [11] H. Idriss et al., *Digest Journal of Nanomaterials & Biostructures* **12**(4), 2017.
- [12] Md Aminul Islam et al., *Journal of Water Process Engineering* **32**, 100911 (2019).
- [13] Navish Kataria, V. K. Garg, *Journal of environmental chemical engineering* **5**(6), 5420–5427 (2017).
- [14] Navish Kataria et al., *Advanced Powder Technology* **27**(4), 1180 (2016).

- [15] Pascal Gottmann et al., *Molecular metabolism* **11**, 145 (2018).
- [16] Gholamreza Kiani et al., *Applied Clay Science* **54**(1), 34 (2011).
- [17] Yosuke Kikuchi et al., *Carbon* **44**(2), 195 (2006).
- [18] A. K. Radzimska, *Materials* **7**(4), 2833 (2014).
- [19] K. Vasanth Kumar, S. Sivanesan, *Dyes and Pigments* **72**(1), 12 (2007).
- [20] Kun-Yi Andrew Lin, Hsuan-Ang Chang, *Chemosphere* **139**, 624 (2015).
- [21] Indra Deo Mall et al., *Colloids and Surfaces A: Physicochemical and Engineering Aspects* **264**(1-3), 17 (2005).
- [22] Venkat S. Mane, P. V. Babu, P. V. Vijay, *Desalination* **273**(2-3), 321 (2011).
- [23] K. Nadafi et al., *Journal of water chemistry and technology* **36**(3), 125 (2014).
- [24] Barun Kumar Nandi, Amit Goswami, Mihir Kumar Purkait, *Journal of hazardous materials* **161**(1), 387 (2009).
- [25] K. Porkodi, K. Kumar, K. Vasanth, *Journal of hazardous materials* **143**(1-2) 311 (2007).
- [26] M. A. Rosa, J. A. Egido, M. C. Márquez, *Applied Clay Science* **182**, 105254 (2019).
- [27] T. Santhi, S. Manonmani, T. Smitha, *Journal of hazardous materials* **179**(1-3), 178 (2010).
- [28] Jean-Pierre Simonin, *Chemical Engineering Journal* **300**, 254 (2016).
- [29] Selene Maria de Arruda Guelli Ulson et al., *Journal of Hazardous Materials* **179**(1-3), 35 (2010).
- [30] Francesc Torrades, Julia García-Montaño, *Dyes and pigments* **100**, 184 (2014).
- [31] S. A. Hosseini et al., *Journal of Alloys and Compounds* **622**, 725 (2015).
- [32] Xianbiao Wang et al., *Colloids and Surfaces A: Physicochemical and Engineering Aspects* **422**, 199 (2013).
- [33] Awanthi Wathukarage et al., *Environmental geochemistry and health* **41**(4), 1647 (2019).
- [34] Aihua Wei et al., *Chemical Engineering Journal* **239**, 141 (2014).
- [35] Feng-Chin Wu, Ru-Ling Tseng, Ruey-Shin Juang, *Chemical Engineering Journal* **150**(2-3), 366009).
- [36] Guiyin Fang et al., *Chemical Engineering Journal* **153**(1-3), 217 (2009).
- [37] Xuejing Wang, Shuwen Yao, Xiaobo Li, *Chinese Journal of Chemistry* **27**(7), 1317 (2009).
- [38] Fan Zhang et al., *Colloids and Surfaces A: Physicochemical and Engineering Aspects* **509**, 474016).
- [39] Fan Zhang et al., *Journal of nanoparticle research* **15**(11), 2034 (2013).
- [40] Randi Zhang et al., *Journal of the Taiwan Institute of Chemical Engineers* **45**(5), 2578 (2014).